COVID

MDPI

Article

KERRA, Mixed Medicinal Plant Extracts, Inhibits SARS-CoV-2 Targets Enzymes and Feline Coronavirus

Supaphorn Seetaha [1,2], Phatcharin Khamplong [1], Panatda Wanaragthai [3], Thitinan Aiebchun [1], Siriluk Ratanabunyong [1], Sucheewin Krobthong [3], Yodying Yingchutrakul [4], Jatuporn Rattanasrisomporn [5] and Kiattawee Choowongkomon [1,2,3,*]

1 Department of Biochemistry, Faculty of Science, Kasetsart University, Bangkok 10900, Thailand; supaporn.se@ku.th (S.S.); phatcharin.p1994@gmail.com (P.K.); thitinan1906@gmail.com (T.A.); ae.med@hotmail.com (S.R.)
2 Kasetsart University Institute for Advanced Studies, Kasetsart University, Bangkok 10900, Thailand
3 Interdisciplinary of Genetic Engineering and Bioinformatics, Graduate School, Kasetsart University, Bangkok 10900, Thailand; panatda.wan@ku.th (P.W.); sucheewin82@gmail.com (S.K.)
4 National Omics Center, National Science and Technology Development Agency, Pathumthani 10110, Thailand; yodying.yin@nstda.or.th
5 Department of Companion Animal Clinical Sciences, Faculty of Veterinary Medicine, Kasetsart University, Bangkok 10900, Thailand; fvetjpn@ku.ac.th
* Correspondence: kiattawee.c@ku.th; Tel.: +66-2-562-5555 (ext. 647729); Fax: +66-2-561-4627

Abstract: The COVID-19 pandemic affects all parameters, especially healthcare professionals, drugs and medical supplies. The KERRA is a mixed medicinal plant capsule that is used for the treatment of patients with high fever, with food and drug administration approved by FDA Thailand. Recently, KERRA showed induced quicker recovery for COVID-19 patients. Therefore, it is possible that some ingredients in KERRA could inhibit SARS-CoV-2. In this study, two important replication-related enzymes in SARS-CoV-2, a main protease and an RNA-dependent RNA polymerase (RdRp), were used to study the effect of KERRA. The results showed that KERRA inhibited the SARS-CoV-2 main protease and SARS-CoV-2 RdRp with IC_{50} values of 49.91 ± 1.75 ng/mL and 36.23 ± 5.23 µg/mL, respectively. KERRA displayed no cytotoxic activity on macrophage cells at concentrations lower than 1 mg/mL and exhibited anti-inflammatory activity. Additionally, KERRA was used against a feline coronavirus (feline infectious peritonitis (FIP)) infection with an EC_{50} value of 134.3 µg/mL. This study supports the potential use of KERRA as a candidate drug for COVID-19.

Keywords: COVID-19 pandemic; KERRA; SARS-CoV-2 main protease; SARS-CoV-2 RNA-dependent RNA polymerase; anti-FIPV activity

check for updates

Citation: Seetaha, S.; Khamplong, P.; Wanaragthai, P.; Aiebchun, T.; Ratanabunyong, S.; Krobthong, S.; Yingchutrakul, Y.; Rattanasrisomporn, J.; Choowongkomon, K. KERRA, Mixed Medicinal Plant Extracts, Inhibits SARS-CoV-2 Targets Enzymes and Feline Coronavirus. *COVID* **2022**, *2*, 621–632. https://doi.org/10.3390/covid2050046

Academic Editor: Francesco Caruso

Received: 26 March 2022
Accepted: 9 May 2022
Published: 16 May 2022

Publisher's Note: MDPI stays neutral with regard to jurisdictional claims in published maps and institutional affiliations.

1. Introduction

Coronavirus disease, or COVID-19, a new disease caused by severe acute respiratory syndrome coronavirus 2 (SARS-CoV-2), was first identified in Wuhan, China, in December 2019 [1]. COVID-19 is a global pandemic and has spread extremely quickly [2], with symptoms such as fever, cough, sore throat, asthma, and lung inflammation [3–5]. In severe cases, respiratory failure and even death can occur [5]. SARS-CoV-2 is easy to infect by contact, droplets, and airborne transmission and all people should protect themselves with hand washing, social distancing 2–4.8 m, and wearing N95 masks [6]. Upon SARS-CoV-2 infection or vaccine induction, both humoral and cellular systems would adapt the immunological protection. Afterward, upon second infection, the body has antibodies and retains the immunological memory resulting in quicker and stronger response [7]. SARS-CoV-2 is a positive-sense single-stranded RNA virus belonging to the Coronaviridae family, *Betacoronavirus* genus, infecting cells of the upper and lower respiratory tract [8]. The enzyme target for COVID-19 treatment is interesting, with two enzymes.

The main protease of SARS-CoV-2 is translated in human host cells to cleave several viral proteins into their active forms [9,10], and RNA-dependent RNA polymerase (RdRp) is used to replicate RNA as the genetic material for SARS-CoV-2 [11,12]. Therefore, further attempts to establish new compounds will inhibit two important SAR-CoV-2 enzyme activities. Several inhibitors in drug discovery have been derived from natural products or medicinal plants, which have been recognized as important sources of new drug discovery. For example, Fah Talai Jone (*Andrographis paniculata*) is one of the medicinal plants used to treat COVID-19 patients in Thailand [13].

The asiatic cholera pandemic during 1826–1837 was occured from India across to Asia, Europe, and the Americas. In Thailand itself, some epidemic crises have also appeared in the past, which considerably damaged the lives and property of the people [14]. In each epidemic, herbal medicines, as basic self-care remedies, became alternative tools to manage the disease. An alternative for Thais to prevent COVID-19 is herbal medicine, particularly from Encyclopaedia of Tak-Ka-Si-La, a volume of Thai wisdom from ancient times. KERRA is an herbal medicine from Tak-Ka-Si-La. KERRA is a mixed nine-ingredient medicinal plant that includes *Dracaena loureiri* Gagnep. [15], *Tarenna hoaensis* Pit. [16], *Schumannianthus dichotomus* (Roxb.) Gagnep. [17], *Momordica cochinchinensis* (Lour.) Spreng. [18], *Citrus aurantifolia* (Christm.) Swingle. [19], *Combretum quadrangulare* Kurz. [20], *Dregea volubilis* Benth. ex Hook.f. [21], *Tiliacora triandra* Diels. [22], and *Tinospora cordifolia* [23]. All nine-ingredient medicinal plants have various pharmacological bioactivities, which are mainly antioxidant and anti-inflammatory.

This study evaluated the inhibition of two important SAR-CoV-2 enzyme activities of KERRA, which exhibited anti-inflammatory activity in RAW264.7 macrophage cells and against feline coronavirus infection. The results demonstrated that KERRA has potent anti-SARS-CoV-2 main protease and anti-SARS-CoV-2 RdRp with no toxicity in cell culture models.

2. Materials and Methods

2.1. Inhibition of the Main Protease of SARS-CoV-2

A sample was prepared of KERRA (Lot no. 048921, Mfg. 21 May 2021, Exp. 20 May 2024 and produce by Vetchakornosot, Bangkok, Thailand) and Fah Talai Jone (*A. paniculata*) at 100 mg/mL in 100% dimethyl sulfoxide as stock solution and stored at −20 °C until used. SARS-CoV-2's main protease inhibition was performed with a fluorogenic assay [24–26]. SARS-CoV-2's main protease gene was synthesis from GenScript company, then expression and purification in our laboratory. The assay was a minor modification of the following steps. Briefly, 200 nM SARS-CoV-2 main protease was preincubated with 10 μg/mL and 100 μg/mL of each inhibitor for 10 min at room temperature. Then, the relative inhibition was started by adding 40 μM fluorogenic substrate (Genscript USA Inc., Piscataway, NJ, USA) to each well. The reaction was monitored at intervals of 10 s for 10 min by fluorescence with excitation at 340 nm and emission at 430 nm (Infinite 200 PRO Microplate Reader, Tecan, Männedorf, Switzerland). The inhibitory effect of recombinant SARS-CoV-2's main protease was compared with lopinavir and ritonavir as commercial drugs for HIV-1 protease inhibition. The IC_{50} measurements of KERRA and *A. paniculate* were determined with 2-fold serial dilutions. All assays were performed in triplicate. The percentage of relative inhibition and IC_{50} values were calculated from the initial velocity (V_0) as Equation (1) using a dose–response curve in GraphPad Prism software, version 8, where V_0 Enzyme is the fluorogenic substrate with the SARS-CoV-2 main protease; V_0 Blank is the fluorogenic substrate without the SARS-CoV-2 main protease; and V_0 Sample is the fluorogenic substrate with sample or commercial drugs.

$$\left[\text{Relative Inhibition } (\%) = \frac{\left[\left(V_o \text{ Enzyme } - V_o \text{ Blank}\right) - \left(V_o \text{ Sample } - V_o \text{ Blank}\right)\right]}{V_o \text{ Enzyme } - V_o \text{Blank}} \times 100\right] \quad (1)$$

2.2. SARS-CoV-2 RNA-Dependent RNA Polymerase Inhibition of KERRA

KERRA and *A. paniculata* were screened for their ability to inhibit the SARS-CoV-2 RdRp enzyme using the RdRp (SAR-CoV-2) homogeneous assay kit (BPS Bioscience: #78109, San Diego, CA, USA) [27]. The RdRp (SAR-CoV-2) gene was synthesized from GenScript company (Genscript USA Inc., Piscataway, NJ, USA), whose expression and purification were conducted in our laboratory. First, 24 ng/µL RdRp enzyme was added to each well for the positive control and the test inhibitors. For the blank, complete RdRp buffer was added. Then, 8-fold diluted RNase inhibitor was added to each well. Subsequently, 100 µg/mL inhibitor was added to each well of the test inhibitors, while the positive control and blank were added to the same solution without inhibitor. All reactions were preincubated for 30 min at room temperature. Then, 2 µL of RdRp reaction mixture, which consisted of diluted digoxigenin-labeled RNA duplex and diluted biotinylated ATP, were mixed and incubated for one hour at 37 °C. Afterward, 10 µL of diluted AlphaLISA anti-digoxigenin acceptor beads (PerkinElmer: #AL113C, Waltham, MA, USA) were added and incubated on a shaker for 30 min at room temperature. Next, 10 µL of diluted streptavidin-conjugated donor beads (PerkinElmer: #6760002S) was added and incubated on a shaker for 30–60 min at room temperature. Finally, the alpha counts were measured using a microplate reader (SPARK® multimode microplate reader, Tecan, Männedorf, Switzerland). All assays were performed in triplicate. The percentage of relative inhibition and IC_{50} values of each sample were analyzed using GraphPad Prism program, version 8.

2.3. Anti-Inflammatory Effect of KERRA in Lipopolysaccharide-Stimulated RAW264.7 Macrophages

RAW264.7 macrophage cells were grown in DMEM supplemented with 10% fetal bovine serum (FBS) and 1% Anti-Anti under a humidified atmosphere of 5% CO_2 at 37 °C. Cells were cultured in a 96-well plate at a density of 1×10^5 cells/well overnight. After incubation, the cells were treated with various concentrations of the sample at 1, 0.5, 0.25 and 0.1 mg/mL and cotreated with 1 µg/mL lipopolysaccharide (LPS) incubated for 24 h at 37 °C with 5% CO_2. Subsequently, 50 µL of media was mixed with 50 µL of Griess reagent and measured by reading absorbance at a wavelength of 540 nm. Cell viability was measured by PrestoBlue™ Cell Viability Reagent (Thermo Fisher Scientific, Carlsbad, CA, USA), and absorbance was read at a wavelength of 570 nm. Data analysis was performed with Equation (2).

$$[\text{anti} - \text{inflammation activity } (\%) = \frac{A_{\text{control}} - A_{\text{test}}}{A_{\text{control}}}] \quad (2)$$

2.4. Anti-FIPV Activity Assay

KERRA was prepared in 100% dimethyl sulfoxide to make a stock solution at 100 mg/mL. The stock solution was serially diluted twofold in DMEM and filtered using Whatman No. 1 filter paper to prepare a working solution before testing. The final concentrations of KERRA ranged from 500 to 31.25 µg/mL. The KERRA stock was kept at −20 °C for further use.

Vero cells (CCL-81™) were seeded in a 24-well plate overnight. For virus preparation, the KERRA at the desired concentrations were incubated with FIPV DF2 strain (ATCC: VR-2004™) at 100 MOI MOI for 1 h at 37 °C in a 5% CO_2 incubator. Subsequently, the cell culture medium was removed and replaced with a KERRA-FIPV mixture. Vero cells were incubated at 37 °C in 5% CO_2 for 2 h. Afterward, the KERRA-FIPV mixture was removed and replaced with 500 µL of maintenance medium. FIPV-infected cells were used as a positive control, while cells treated with DMSO were used as a negative control. The inoculated cells were continuously incubated at 37 °C in 5% CO_2 for 72 h. The FIPV was collected by freeze–thawing 3 times and centrifuged to separate the cells debris. The FIPV RNA was extracted by Omega Bio-tek, Inc. (Norcross, GA, USA) kit. The viral copy number of each sample was determined using quantitative real-time RT–PCR (qRT–PCR) (Bio-Rad,

Shinagawa, Tokyo, Japan). The effective concentration that attained a 50% decrease in viral replication was defined as the EC50 value.

2.5. Phytochemical Profile Analysis Using LC–MS/MS

Phytochemical profiling analysis was prepared using a previous protocol with minor modifications [28]. Briefly, the extract powder (0.7 g) was mixed with 14 mL of ethanol. The suspension was incubated for 72 h at 8 °C with a shaker at 100 rpm. Then, the solution was centrifuged at 14,000× *g* for 30 min at 8 °C. SPE with the extraction manifold system was used to clean the clear upper solution. SPE was preconditioned using 20 mL of acetonitrile and equilibrated with 50 mL of water. The supernatants were loaded on the equilibrated SPE and eluted with 99% acetonitrile/water. The eluted fractions were evaporated under a vacuum using rotatory evaporation. To confirm the phytochemical content, the experiments were conducted in 3 biological replications. The samples were reconstituted in 1000 µL of methanol and diluted with 1000 µL of 0.2% formic acid/water before being subjected to LC–MS/MS analysis. Quality control of the samples was conducted to confirm the reproducibility data, and LC–MS/MS was used to determine the total ion intensity of all of the identified compounds from three independent extraction batches and three technical injections.

The acquired raw MS files were processed with Compound Discoverer software, version 3.1 (Thermo Fisher Scientific, Waltham, MA, USA), to identify phytochemicals. Peak identification, peak alignment, and peak feature extraction were all conducted in positive mode on the data. The retention time (RT) and mass-to-charge ratio (m/z) of different injections were determined according to the retention time deviation of 0.5 min and the mass deviation of 5 ppm. Then, peak extraction was performed according to the set information and adduct information: mass deviation = 5 ppm, signal strength deviation = 30%, signal-to-noise ratio = 2, and fine isotopic pattern matching >90% of the precursor and the characteristic product ions. Additionally, the peak area was quantified. The target m/z ions were then integrated to predict the molecular formula, which was compared to the mzCloud (https://www.mzcloud.org; accessed date 23 March 2022) and ChemSpider (http://www.chemspider.com; accessed date 23 March 2022) online databases for the identification and confirmation of the compounds. Furthermore, structural elucidation and transformations were suggested for each chromatographic peak by the Fragment Ion Search^{TM} (FISh) function. The FISh coverage score was calculated, and fragments on the MS/MS spectrum were autoannotated with structure, molecular weight, and elemental composition. Among candidate metabolites obtained from mzCloud and ChemSpider with FISh, the highest MS/MS coverage scores were selected for annotation. The candidate metabolites with annotation and with mzClound best match scores > 60 and FISh coverage > 20 or area > 1×10^9 AU were reported.

3. Results

3.1. Inhibition of the Main Protease of SARS-CoV-2 by KERRA

The main protease of SARS-CoV-2 is one of the main enzymes that plays a crucial role in viral replication and is highly conserved; it is one of the most attractive therapeutic targets for SARS-CoV-2 inhibition. This protein has been a target for the development of drugs and for virtual screening in several projects [24,29–31]. Lopinavir and ritonavir were the first two drugs suggested for use in the treatment of COVID-19 patients [32–34]. Furthermore, Fah Talai Jone (*A. paniculata*) was one herbal medicine recommended for use by the FDA in Thailand as an alternative drug [13,35,36]. The effects of these compounds were tested against the SARS-CoV-2 main protease. The fluorogenic assay was used to measure the proteolytic activity of the recombinant SARS-CoV-2 main protease [24,37,38]. The relative inhibition of KERRA, *A. paniculata*, lopinavir and ritonavir was determined at two concentrations: 10 µg/mL and 100 µg/mL. The results showed the dose-dependent inhibition of SARS-CoV-2 main protease by all tested compounds. At 10 µg/mL, each sample showed enzyme proteolytic inhibition lower than 50%, except for KERRA, which showed 76.46% inhibition. The activity at 100 µg/mL of each sample represented inhibition of more

than 50%, except for *A. paniculata,* while KERRA resulted in complete inhibition (Figure 1). The IC_{50} values of all compounds were determined for comparison. The IC_{50} values of lopinavir and ritonavir were 77.03 ± 8.51 μg/mL (122.50 μM) and 23.39 ± 2.52 μg/mL (32.44 μM), respectively (Figure 2a,b). These values are similar to those previously reported; the IC_{50} values of lopinavir were more than 40 μg/mL (>60 μM), and those of ritonavir were more than 15 μg/mL (>20 μM) [35,36], indicating the reliability of our assay method. Furthermore, the IC_{50} value of the *A. paniculata* extract was 29.94 ± 8.51 μg/mL (Figure 2c). This report is the first of the IC_{50} of *A. paniculata* extract against the main protease since it was previously proposed that andrographolide from *A. paniculata* extract targeted this main protease by molecular docking [13]. Interestingly, KERRA showed an IC_{50} value of 46.35 ± 4.89 ng/mL (Figure 2d), which was 650 times lower than that of the *A. paniculata* extract. These data indicated that KERRA is a candidate inhibitor of the main protease SARS-CoV-2.

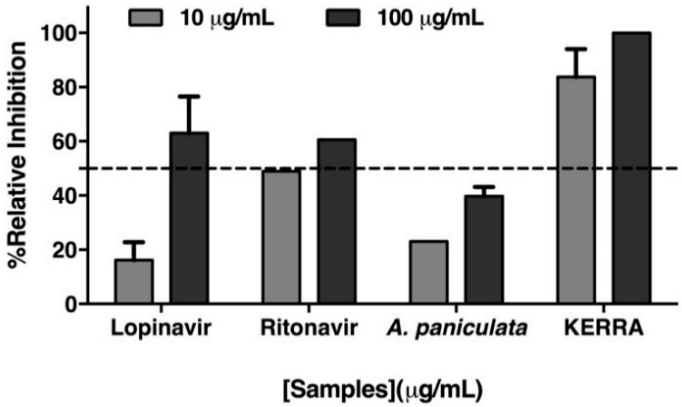

Figure 1. Relative inhibition of the main protease of SARS-CoV-2 with 10 and 100 μg/mL lopinavir, ritonavir, KERRA and *A. paniculata*.

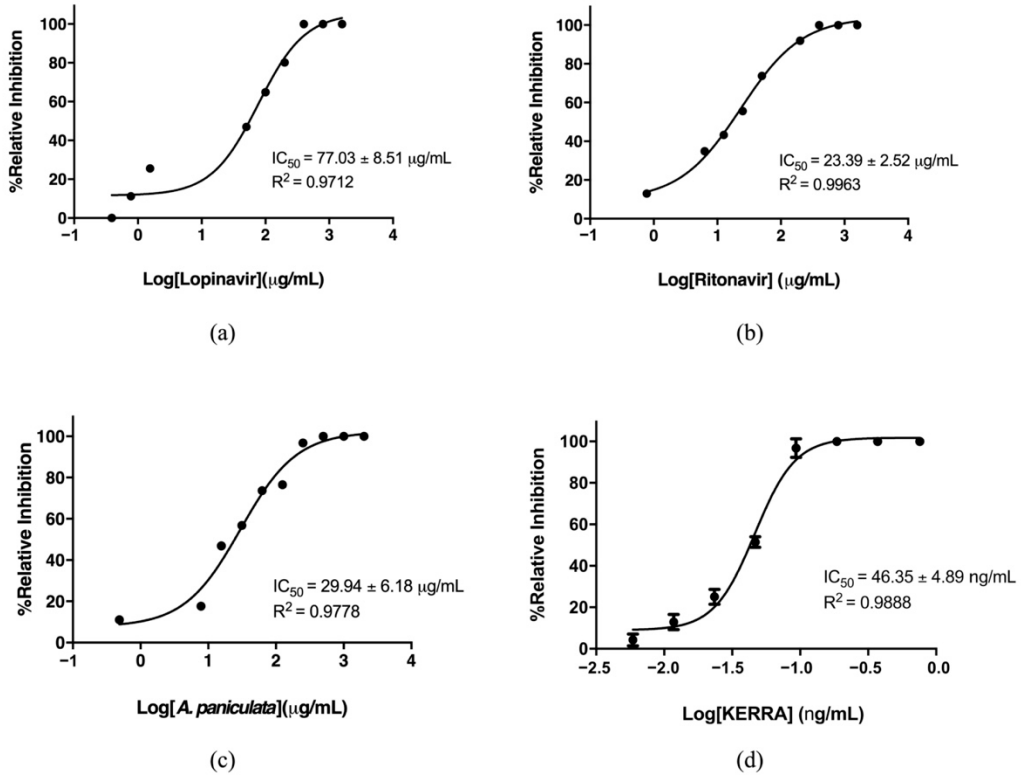

Figure 2. IC_{50} of KERRA against the main protease of SARS-CoV-2 with (**a**) lopinavir, (**b**) ritonavir, (**c**) *A. paniculate* and (**d**) KERRA.

3.2. KERRA Inhibition of RdRp (SARS-CoV-2)

The other important enzyme for inhibiting virus replication is an RNA-dependent RNA polymerase (RdRp). As previously reported, favipiravir effectively inhibited RdRp (SARS-CoV-2) activity in viral cell culture [37,38]. However, favipiravir is a prodrug, which is a molecule with little or no pharmacological activity, that is converted into the active parent drug in vivo by enzymatic or chemical reactions. Therefore, the inhibitory activity of the SARS-CoV-2 RdRp assay was used to determine the effect of KERRA. The inhibitory activities of KERRA, *A. paniculate*, and favipiravir were tested at 100 μg/mL using an RdRp (SARS-CoV-2) homogeneous assay kit [27]. Interestingly, the results showed that KERRA was the most effective against SARS-CoV-2 RdRp among all compounds, with 57.16% efficacy (Figure 3a). This enzymatic inhibition result for favipiravir is not surprising since it is a prodrug form. It is not fully active until it is metabolized by cells to activate favipiravir-ribofuranosyl-5′-triphosphate (favipiravir-RTP). KERRA was evaluated for IC_{50} values and showed inhibitory activity against RdRp (SARS-CoV-2), with an IC_{50} value of 36.23 ± 5.23 μg/mL. The IC_{50} values of RdRp (SARS-CoV-2), such as remdesivir (2.58 ± 0.27 μM), lycorine (1.41 ± 0.26 μM), adefovir dipivoxil (3.78 ± 0.87 μM), emtricitabine (15.38 ± 3.60 μM) and favipiravir (61.88 μM), have been mostly investigated in cell base assays [39–41]. Therefore, this study is the first report of the IC_{50} of RdRp (SARS-CoV-2) with an enzyme activity assay.

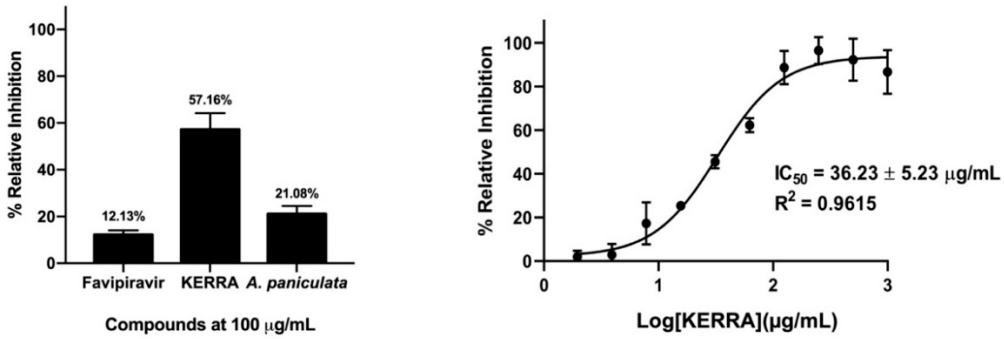

Figure 3. (**a**) The percentage of relative inhibition compared among favipiravir, KERRA and *A. paniculata* at 100 μg/mL against RdRp (SARS-CoV-2) activity. (**b**) The IC_{50} of KERRA against RdRp (SARS-CoV-2) activity.

3.3. Effect of KERRA on Anti-Inflammation Activity

First, for the cytotoxicity assay, RAW 264.7 macrophage cells were treated for 24 h with various concentrations of KERRA at 1, 0.5, 0.25 and 0.1 mg/mL. The results showed that the RAW 264.7 macrophage cells treated with 1, 0.5, 0.25 and 0.1 mg/mL KERRA had cell viability values of 95.51%, 96.94%, 92.65% and 91.16%, respectively. Cell viability greater than 80% indicated that KERRA was not toxic to cells (Figure 4a).

The anti-inflammatory activity of macrophage cells after treatment with KERRA for 24 h at concentrations of 1, 0.5, 0.25 and 0.1 mg/mL was investigated for the production of nitric oxide (NO) using Griess reagent. In this experiment, 1 μg/mL LPS and 65 μg/mL diclofenac were used as negative and positive controls, respectively. The results showed that 1 mg/mL KERRA had the highest anti-inflammatory activity at 79.66%, followed by 0.5, 0.25, and 0.1 mg/mL KERRA at 59.46%, 34.99% and 7.87%, respectively (Figure 4b). This result indicated that KERRA could have anti-inflammatory activity.

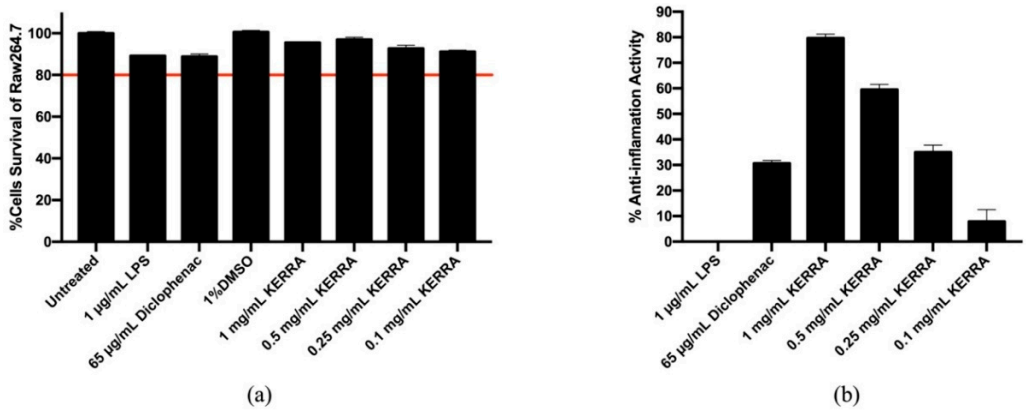

Figure 4. Cell viability and anti-inflammatory activity of RAW264.7 macrophage cells. (**a**) Cell viability after treatment with KERRA using PrestoBlue™ Cell Viability Reagent. (**b**) Anti-inflammatory activity of RAW264.7 macrophage cells after treatment for 24 h with various concentrations of KERRA.

3.4. Anti-FIPV Activity

To test whether KERRA can be effective at the cellular level, feline coronavirus was used as a model for studying inhibition since it has homological structures of the main protease and RdRp to SAR-COV-2, and it can be performed in the BSL2 laboratory. Anti-FIP virus activity was assessed by qRT–PCR to quantify the effect of inhibition by determining the number of FIPV copies in the cells. Infected Vero cells found FIP virus at 9×10^6 copy numbers after 3 days of infection. The Vero cells treated with 1 mg/mL KERRA found that the amount of FIP virus decreases to 6×10^5 copy numbers (Figure 5a). Preliminary experiments of EC50 insinuate that coculture with KERRA decreased the amount of FIPV in Vero cells, yielding an EC50 value of 134.3 μg/mL (Figure 5b). This result indicates that KERRA could inhibit virus propagation in Vero cells.

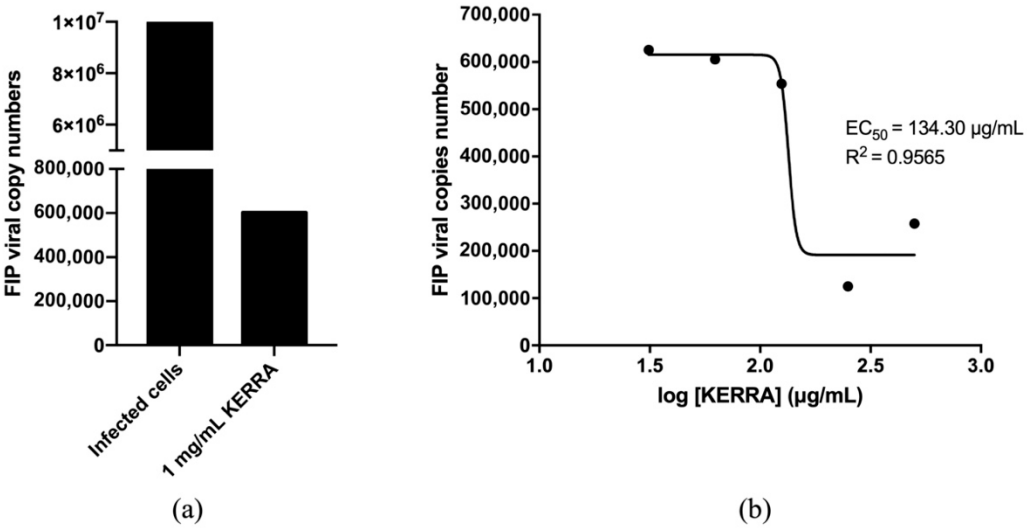

Figure 5. Copy numbers of Vero cells infected with FIPV. (**a**) A total of 1 mg/mL KERRA was incubated with FIPV before infection compare with infected cells. (**b**) KERRA showed an EC_{50} value of 134.3 μg/mL against FIP virus infection of Vero cells.

3.5. Phytochemical Profiling and Qualitative Metabolite Analysis

The accuracy of phytochemical profile data depends greatly on biological sampling and LC–MS/MS instrument performance. To examine whether the instrument is in good operating condition and whether the sample preparation and method applied were appropriate, the TIC of all injections is shown in Figure 6. The TIC of independent batches and technical replicates revealed consistency and reproducibility. The highest peak at

approximately 6.6 min was shown in 9 LC–MS runs. Additionally, this peak exhibited good symmetry and was consistent across the three batches of the experiments (compound coefficient of variance per sample batch as 4%). Additionally, the TIC of all the detected metabolites in the 9 LC runs revealed that their profiles were extremely comparable in terms of elution times and intensity values, indicating consistency and reproducibility in batches at the overall level. The identification of metabolites by LC–MS/MS with HCD in positive mode is well-established. A total of 414 annotated phytochemical species were identified (Supplementary Table S1). Table 1 lists the top ten phytochemicals.

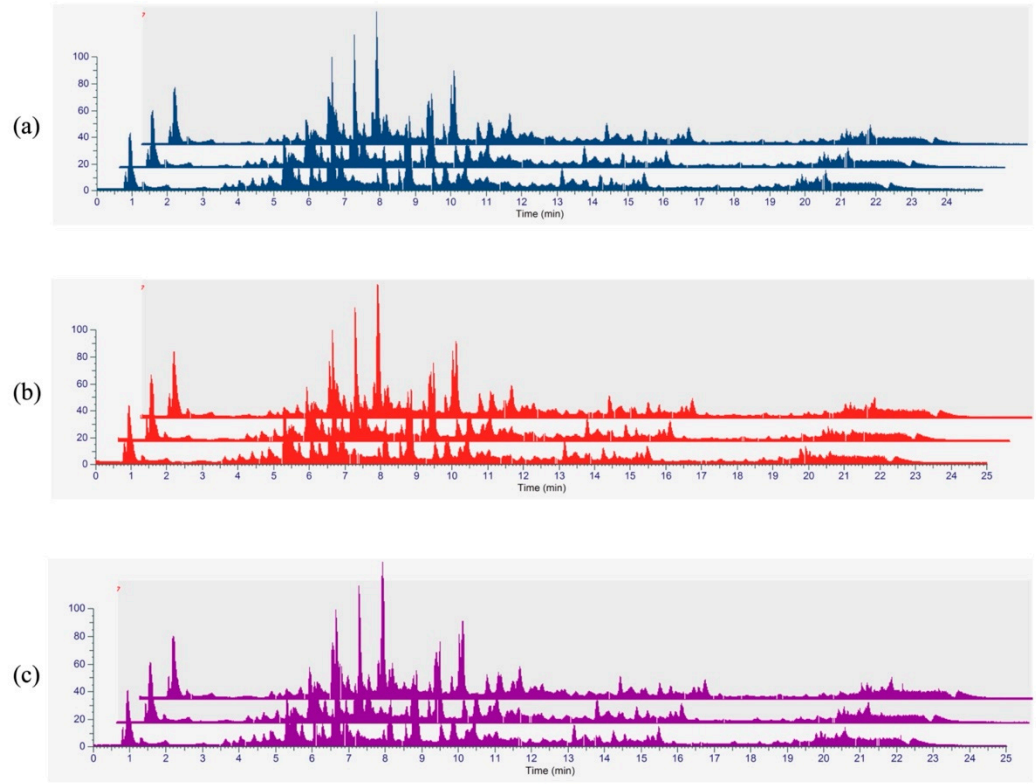

Figure 6. LC–MS/MS phytochemical profiles of KERRA. Aligned TIC profiles of KERRA in three LC runs of 25 min. (**a**) KERRA batch 1; (**b**) KERRA batch 2; and (**c**) KERRA batch 3. The units of the X-axis and Y-axis are minutes and percentage intensity abundance, respectively.

Table 1. List of high-abundance phytochemicals detected in KERRA.

List	Name	Formula	Molecular Weight (Da)	Area
1	2-Methoxy-9H-xanthen-9-one	C_{14} H_{10} O_3	226.0594	7.43×10^9
2	Isorhapontigenin	C_{15} H_{14} O_4	276.0960	7.36×10^9
3	Betaine	C_5 H_{11} N O_2	117.0776	6.84×10^9
4	-	C_{20} H_{28} O_4	314.1837	6.81×10^9
5	trans-Anethole	C_{10} H_{12} O	148.0869	4.82×10^9
6	Eicosatetraynoic acid	C_{20} H_{24} O_2	296.1734	4.05×10^9
7	NP-020078	C_{17} H_{28} O_3	302.1847	3.28×10^9
8	NP-003294	C_{18} H_{16} O_7	344.0850	3.09×10^9
9	-	C_{20} H_{30} O_5	332.1946	2.88×10^9
10	N1-(3-chlorophenyl)-2-[2-(trifluoromethyl)-4-quinolyl]hydrazine-1-carboxamide	C_{17} H_{12} Cl F_3 N_4 O	380.0672	2.37×10^9

KERERA identified three major components: 2-methoxy-9H-xanthen-9-one, isorhapontigenin, and betaine. The presence of these annotated compounds was confirmed and validated

using their respective accurate mass, experimental and calculated *m/z*, molecular formula, precursor mass error, MS2 fragmentation pattern, and well-known database matching.

4. Discussion

In vitro studies of the inhibitory activity of the SARS-CoV-2 main protease of KERRA found that the IC_{50} of KERRA was 49.91 ± 1.75 ng/mL, which was lower than that of ritonavir and lopinavir, which are used for COVID-19. The inhibitory activity of RdRp (SARS-CoV-2) and of KERRA compared with favipiravir (prodrug form) at 100 µg/mL showed that KERRA showed relative inhibition against RdRp (SARS-CoV-2) activity better than favipiravir by approximately five-fold, representing an IC_{50} value of 36.23 ± 5.23 µg/mL. However, this study used favipiravir in a prodrug form, which is not fully active until it is metabolized by cells to activate favipiravir-ribofuranosyl-5′-triphosphate (favipiravir-RTP) [42]. Therefore, the RdRp (SARS-CoV-2) inhibition of favipiravir assay showed low inhibitory activity.

The determination of cytotoxicity to RAW264.7 cells found that the cell viability was higher than 80% at a high concentration of 1 mg/mL KERRA, indicating that KERRA is not toxic to cells. However, 1 mg/mL KERRA was the best concentration, exhibiting the highest anti-inflammatory activity. The anti-inflammatory activity of diclofenac is lower than that of KERRA because this experiment used a concentration lower than the sample based on the dose recommended [43]. Moreover, Vero cells treated with KERRA showed a decrease in FIP virus copy number, confirming that KERRA could reduce FIP viral infection. Our results are related to a previous study of 9H-xanthen derivatives [44], and isorhapontigenin [45] could have antiviral activity. Therefore, KERRA is a potent mixed herb against SARS-CoV-2 virus infection.

With additional LC–MS/MS results, KERRA identified 2-methoxy-9H-xanthen-9-one, which is one of the major xanthones with a wide range of biological activities [46]. The second major compound is isorhapontigenin, a bioavailable dietary polyphenol that plays a role in epithelial cell anti-inflammation through a corticosteroid-independent mechanism and that inhibits the PI3K/Akt pathway, which is insensitive to corticosteroids [47]. Moreover, isorhapontigenin has exhibited activity on SARS-CoV-2 virus-infected Vero cells [48]. Betaine is a stable and nontoxic trimethylglycine that is widely distributed in animals, plants, and microorganisms. Betaine, as an osmoprotectant and a methyl group donor, has displayed anti-inflammatory effects in various diseases [49]. These effects were associated with protecting SAA metabolism from oxidative stress, inhibiting NF-κB and NLRP3 inflammasome activity, regulating energy metabolism, and mitigating ER stress and apoptosis [50]. Three major compounds in KERRA are available in natural products and have been found to have anti-inflammatory functions.

5. Conclusions

KERRA is a combination of nine medicinal plants that showed inhibitory activity against the main protease of SARS-CoV-2 and RdRp (SARS-CoV-2) in assays with IC_{50} values of 49.91 ± 1.75 ng/mL and 36.23 ± 5.23 µg/mL, respectively. KERRA was nontoxic to RAW264.7 cells at concentrations lower than 1 mg/mL and exhibited the highest anti-inflammatory activity at 79.66%. FIP virus infection showed an EC50 value of 134.3 µg/mL. Furthermore, the major compounds in KERRA were found in medicinal plants, and they have a bioactive role that could treat many diseases as their main anti-inflammatory function. Therefore, KERRA is a candidate for drug treatment of COVID-19, and further study is recommended with animal models and clinical trials. However, Thai medicinal plants could be most beneficial to use and could be further developed as commercial drugs.

6. Patents

There are no intellectual patents issued on any of the investigational ingredients, as these are already freely available and can be purchased over the counter.

Supplementary Materials: The following are available online at https://www.mdpi.com/article/10.3390/covid2050046/s1, Table S1: Phytochemical Profiles of KERRA extracts.

Author Contributions: Conceptualization and Writing—Editing, K.C. and J.R.; Writing—Review and Writing—Original Draft Preparation, S.S.; Inhibition of SARS-CoV-2 main protease experiment, P.K.; Inhibition of SARS-CoV-2 RNA dependent RNA polymerase experiment, T.A.; Anti-inflammation activity experiment, P.W.; Anti-FIPV infection experiment, S.R.; LC–MS/MS experiment, S.K. and Y.Y. All authors have read and agreed to the published version of the manuscript.

Funding: This research was funded by Kasetsart University Research and Development Institute, KURDI (FF (KU) 25.64).

Institutional Review Board Statement: Not applicable.

Informed Consent Statement: Not applicable.

Data Availability Statement: Not applicable.

Acknowledgments: This work was financially supported by the Office of the Ministry of Higher Education, Science, Research and Innovation; the Thailand Science Research and Innovation through the Kasetsart University Reinventing University Program 2021; and by the Kasetsart University Research and Development Institute, KURDI (FF (KU) 25.64).

Conflicts of Interest: The authors declare that they have no conflict of interest.

References

1. Lu, H.; Stratton, C.W.; Tang, Y.W. Outbreak of pneumonia of unknown etiology in Wuhan, China: The mystery and the miracle. *J. Med. Virol.* **2020**, *92*, 401–402. [CrossRef] [PubMed]
2. Lai, C.C.; Shih, T.P.; Ko, W.C.; Tang, H.J.; Hsueh, P.R. Severe acute respiratory syndrome coronavirus 2 (SARS-CoV-2) and coronavirus disease-2019 (COVID-19): The epidemic and the challenges. *Int. J. Antimicrob. Agents* **2020**, *55*, 105924. [CrossRef] [PubMed]
3. Harrison, A.G.; Lin, T.; Wang, P. Mechanisms of SARS-CoV-2 Transmission and Pathogenesis. *Trends Immunol.* **2020**, *41*, 1100–1115. [CrossRef]
4. Singh, A.K.; Gupta, R.; Ghosh, A.; Misra, A. Diabetes in COVID-19: Prevalence, pathophysiology, prognosis and practical considerations. *Diabetes Metab. Syndr.* **2020**, *14*, 303–310. [CrossRef] [PubMed]
5. Sanyaolu, A.; Okorie, C.; Marinkovic, A.; Patidar, R.; Younis, K.; Desai, P.; Hosein, Z.; Padda, I.; Mangat, J.; Altaf, M. Comorbidity and its Impact on Patients with COVID-19. *SN Compr. Clin. Med.* **2020**, *2*, 1069–1076. [CrossRef] [PubMed]
6. Priyanka, O.P.C.; Singh, I.; Patra, G. Aerosol transmission of SARS-CoV-2: The unresolved paradox. *Travel Med. Infect. Dis.* **2020**, *37*, 101869. [CrossRef]
7. Priyanka, O.P.C.; Singh, I. Protective immunity against COVID-19: Unravelling the evidences for humoral vs. cellular components. *Travel Med. Infect. Dis.* **2021**, *39*, 101911. [CrossRef]
8. Coronaviridae Study Group of the International Committee on Taxonomy of Viruses. The species Severe acute respiratory syndrome-related coronavirus: Classifying 2019-nCoV and naming it SARS-CoV-2. *Nat. Microbiol.* **2020**, *5*, 536–544. [CrossRef]
9. Wang, Y.C.; Yang, W.H.; Yang, C.S.; Hou, M.H.; Tsai, C.L.; Chou, Y.Z.; Hung, M.C.; Chen, Y. Structural basis of SARS-CoV-2 main protease inhibition by a broad-spectrum anti-coronaviral drug. *Am. J. Cancer Res.* **2020**, *10*, 2535–2545.
10. Razali, R.; Asis, H.; Budiman, C. Structure-Function Characteristics of SARS-CoV-2 Proteases and Their Potential Inhibitors from Microbial Sources. *Microorganisms* **2021**, *9*, 2481. [CrossRef]
11. Jiang, Y.; Yin, W.; Xu, H.E. RNA-dependent RNA polymerase: Structure, mechanism, and drug discovery for COVID-19. *Biochem. Biophys. Res. Commun.* **2021**, *538*, 47–53. [CrossRef] [PubMed]
12. Hillen, H.S. Structure and function of SARS-CoV-2 polymerase. *Curr. Opin. Virol.* **2021**, *48*, 82–90. [CrossRef] [PubMed]
13. Sa-Ngiamsuntorn, K.; Suksatu, A.; Pewkliang, Y.; Thongsri, P.; Kanjanasirirat, P.; Manopwisedjaroen, S.; Charoensutthivarakul, S.; Wongtrakoongate, P.; Pitiporn, S.; Chaopreecha, J.; et al. Anti-SARS-CoV-2 Activity of Andrographis paniculata Extract and Its Major Component Andrographolide in Human Lung Epithelial Cells and Cytotoxicity Evaluation in Major Organ Cell Representatives. *J. Nat. Prod.* **2021**, *84*, 1261–1270. [CrossRef]
14. Daly, W.J. The black cholera comes to the central valley of America in the 19th century—1832, 1849, and later. *Trans. Am. Clin. Climatol. Assoc.* **2008**, *119*, 143–152. [PubMed]
15. Sun, J.; Liu, J.N.; Fan, B.; Chen, X.N.; Pang, D.R.; Zheng, J.; Zhang, Q.; Zhao, Y.F.; Xiao, W.; Tu, P.F.; et al. Phenolic constituents, pharmacological activities, quality control, and metabolism of Dracaena species: A review. *J. Ethnopharmacol.* **2019**, *244*, 112138. [CrossRef] [PubMed]
16. Yang, X.W.; Wang, J.S.; Wang, Y.H.; Xiao, H.T.; Hu, X.J.; Mu, S.Z.; Ma, Y.L.; Lin, H.; He, H.P.; Li, L.; et al. Tarennane and tarennone, two novel chalcone constituents from Tarenna attenuata. *Planta Med.* **2007**, *73*, 496–498. [CrossRef]

17. Rob, M.M.; Hossen, K.; Iwasaki, A.; Suenaga, K.; Kato-Noguchi, H. Phytotoxic Activity and Identification of Phytotoxic Substances from Schumannianthus dichotomus. *Plants* **2020**, *9*, 102. [CrossRef] [PubMed]
18. Tsoi, A.Y.; Ng, T.B.; Fong, W.P. Immunomodulatory activity of a chymotrypsin inhibitor from Momordica cochinchinensis seeds. *J. Pept. Sci.* **2006**, *12*, 605–611. [CrossRef]
19. Liu, W.; Zheng, W.; Cheng, L.; Li, M.; Huang, J.; Bao, S.; Xu, Q.; Ma, Z. Citrus fruits are rich in flavonoids for immunoregulation and potential targeting ACE2. *Nat. Prod. Bioprospect.* **2022**, *12*, 4. [CrossRef]
20. Banskota, A.H.; Tezuka, Y.; Adnyana, I.K.; Xiong, Q.; Hase, K.; Tran, K.Q.; Tanaka, K.; Saiki, I.; Kadota, S. Hepatoprotective effect of Combretum quadrangulare and its constituents. *Biol. Pharm. Bull.* **2000**, *23*, 456–460. [CrossRef]
21. Itthiarbha, A.; Phitak, T.; Sanyacharernkul, S.; Pothacharoen, P.; Pompimon, W.; Kongtawelert, P. Polyoxypregnane glycoside from Dregea volubilis extract inhibits IL-1beta-induced expression of matrix metalloproteinase via activation of NF-kappaB in human chondrocytes. *In Vitro Cell. Dev. Biol. Anim.* **2012**, *48*, 43–53. [CrossRef] [PubMed]
22. Sureram, S.; Senadeera, S.P.; Hongmanee, P.; Mahidol, C.; Ruchirawat, S.; Kittakoop, P. Antimycobacterial activity of bisbenzylisoquinoline alkaloids from Tiliacora triandra against multidrug-resistant isolates of Mycobacterium tuberculosis. *Bioorg. Med. Chem. Lett.* **2012**, *22*, 2902–2905. [CrossRef] [PubMed]
23. Sharma, P.; Dwivedee, B.P.; Bisht, D.; Dash, A.K.; Kumar, D. The chemical constituents and diverse pharmacological importance of Tinospora cordifolia. *Heliyon* **2019**, *5*, e02437. [CrossRef]
24. Ihssen, J.; Faccio, G.; Yao, C.; Sirec, T.; Spitz, U. Fluorogenic in vitro activity assay for the main protease M(pro) from SARS-CoV-2 and its adaptation to the identification of inhibitors. *STAR Protoc.* **2021**, *2*, 100793. [CrossRef] [PubMed]
25. Garcia-Echeverria, C.; Rich, D.H. New intramolecularly quenched fluorogenic peptide substrates for the study of the kinetic specificity of papain. *FEBS Lett.* **1992**, *297*, 100–102. [CrossRef]
26. Chen, S.; Chen, L.L.; Luo, H.B.; Sun, T.; Chen, J.; Ye, F.; Cai, J.H.; Shen, J.K.; Shen, X.; Jiang, H.L. Enzymatic activity characterization of SARS coronavirus 3C-like protease by fluorescence resonance energy transfer technique. *Acta Pharmacol. Sin.* **2005**, *26*, 99–106. [CrossRef]
27. Wang, Q.; Wu, J.; Wang, H.; Gao, Y.; Liu, Q.; Mu, A.; Ji, W.; Yan, L.; Zhu, Y.; Zhu, C.; et al. Structural Basis for RNA Replication by the SARS-CoV-2 Polymerase. *Cell* **2020**, *182*, 417–428.e13. [CrossRef]
28. Yingchutrakul, Y.; Sittisaree, W.; Mahatnirunkul, T.; Chomtong, T.; Tulyananda, T.; Krobthong, S. Cosmeceutical Potentials of Grammatophyllum speciosum Extracts: Anti-Inflammations and Anti-Collagenase Activities with Phytochemical Profile Analysis Using an Untargeted Metabolomics Approach. *Cosmetics* **2021**, *8*, 116. [CrossRef]
29. Huff, S.; Kummetha, I.R.; Tiwari, S.K.; Huante, M.B.; Clark, A.E.; Wang, S.; Bray, W.; Smith, D.; Carlin, A.F.; Endsley, M.; et al. Discovery and Mechanism of SARS-CoV-2 Main Protease Inhibitors. *J. Med. Chem.* **2022**, *65*, 2866–2879. [CrossRef]
30. Li, Z.; Li, X.; Huang, Y.Y.; Wu, Y.; Liu, R.; Zhou, L.; Lin, Y.; Wu, D.; Zhang, L.; Liu, H.; et al. Identify potent SARS-CoV-2 main protease inhibitors via accelerated free energy perturbation-based virtual screening of existing drugs. *Proc. Natl. Acad. Sci. USA* **2020**, *117*, 27381–27387. [CrossRef]
31. Amporndanai, K.; Meng, X.; Shang, W.; Jin, Z.; Rogers, M.; Zhao, Y.; Rao, Z.; Liu, Z.J.; Yang, H.; Zhang, L.; et al. Inhibition mechanism of SARS-CoV-2 main protease by ebselen and its derivatives. *Nat. Commun.* **2021**, *12*, 3061. [CrossRef] [PubMed]
32. Drozdzal, S.; Rosik, J.; Lechowicz, K.; Machaj, F.; Kotfis, K.; Ghavami, S.; Los, M.J. FDA approved drugs with pharmacotherapeutic potential for SARS-CoV-2 (COVID-19) therapy. *Drug Resist. Updat.* **2020**, *53*, 100719. [CrossRef] [PubMed]
33. Magro, P.; Zanella, I.; Pescarolo, M.; Castelli, F.; Quiros-Roldan, E. Lopinavir/ritonavir: Repurposing an old drug for HIV infection in COVID-19 treatment. *Biomed. J.* **2021**, *44*, 43–53. [CrossRef] [PubMed]
34. Group, R.C. Lopinavir-ritonavir in patients admitted to hospital with COVID-19 (RECOVERY): A randomised, controlled, open-label, platform trial. *Lancet* **2020**, *396*, 1345–1352. [CrossRef]
35. Ma, C.; Sacco, M.D.; Hurst, B.; Townsend, J.A.; Hu, Y.; Szeto, T.; Zhang, X.; Tarbet, B.; Marty, M.T.; Chen, Y.; et al. Boceprevir, GC-376, and calpain inhibitors II, XII inhibit SARS-CoV-2 viral replication by targeting the viral main protease. *bioRxiv* **2020**. [CrossRef]
36. Ma, C.; Tan, H.; Choza, J.; Wang, Y.; Wang, J. Validation and invalidation of SARS-CoV-2 main protease inhibitors using the Flip-GFP and Protease-Glo luciferase assays. *Acta Pharm. Sin. B* **2022**, *12*, 1636–1651. [CrossRef]
37. Wang, X.; Sacramento, C.Q.; Jockusch, S.; Chaves, O.A.; Tao, C.; Fintelman-Rodrigues, N.; Chien, M.; Temerozo, J.R.; Li, X.; Kumar, S.; et al. Combination of antiviral drugs inhibits SARS-CoV-2 polymerase and exonuclease and demonstrates COVID-19 therapeutic potential in viral cell culture. *Commun. Biol.* **2022**, *5*, 154. [CrossRef]
38. Driouich, J.S.; Cochin, M.; Lingas, G.; Moureau, G.; Touret, F.; Petit, P.R.; Piorkowski, G.; Barthelemy, K.; Laprie, C.; Coutard, B.; et al. Favipiravir antiviral efficacy against SARS-CoV-2 in a hamster model. *Nat. Commun.* **2021**, *12*, 1735. [CrossRef]
39. Jin, Y.H.; Min, J.S.; Jeon, S.; Lee, J.; Kim, S.; Park, T.; Park, D.; Jang, M.S.; Park, C.M.; Song, J.H.; et al. Lycorine, a non-nucleoside RNA dependent RNA polymerase inhibitor, as potential treatment for emerging coronavirus infections. *Phytomedicine* **2021**, *86*, 153440. [CrossRef]
40. Min, J.S.; Kwon, S.; Jin, Y.H. SARS-CoV-2 RdRp Inhibitors Selected from a Cell-Based SARS-CoV-2 RdRp Activity Assay System. *Biomedicines* **2021**, *9*, 996. [CrossRef]
41. Fan, S.; Xiao, D.; Wang, Y.; Liu, L.; Zhou, X.; Zhong, W. Research progress on repositioning drugs and specific therapeutic drugs for SARS-CoV-2. *Future Med. Chem.* **2020**, *12*, 1565–1578. [CrossRef] [PubMed]

42. Furuta, Y.; Komeno, T.; Nakamura, T. Favipiravir (T-705), a broad spectrum inhibitor of viral RNA polymerase. *Proc. Jpn. Acad. Ser. B Phys. Biol. Sci.* **2017**, *93*, 449–463. [CrossRef] [PubMed]
43. Woranam, K.; Senawong, G.; Utaiwat, S.; Yunchalard, S.; Sattayasai, J.; Senawong, T. Anti-inflammatory activity of the dietary supplement Houttuynia cordata fermentation product in RAW264.7 cells and Wistar rats. *PLoS ONE* **2020**, *15*, e0230645. [CrossRef] [PubMed]
44. Maia, M.; Resende, D.; Duraes, F.; Pinto, M.M.M.; Sousa, E. Xanthenes in Medicinal Chemistry—Synthetic strategies and biological activities. *Eur. J. Med. Chem.* **2021**, *210*, 113085. [CrossRef] [PubMed]
45. Chan, C.N.; Trinite, B.; Levy, D.N. Potent Inhibition of HIV-1 Replication in Resting CD4 T Cells by Resveratrol and Pterostilbene. *Antimicrob. Agents Chemother.* **2017**, *61*. [CrossRef]
46. Markowicz, J.; Uram, L.; Sobich, J.; Mangiardi, L.; Maj, P.; Rode, W. Antitumor and anti-nematode activities of alpha-mangostin. *Eur. J. Pharmacol.* **2019**, *863*, 172678. [CrossRef]
47. Yeo, S.C.M.; Fenwick, P.S.; Barnes, P.J.; Lin, H.S.; Donnelly, L.E. Isorhapontigenin, a bioavailable dietary polyphenol, suppresses airway epithelial cell inflammation through a corticosteroid-independent mechanism. *Br. J. Pharmacol.* **2017**, *174*, 2043–2059. [CrossRef]
48. Fang, J.; Wu, Q.; Ye, F.; Cai, C.; Xu, L.; Gu, Y.; Wang, Q.; Liu, A.L.; Tan, W.; Du, G.H. Network-Based Identification and Experimental Validation of Drug Candidates Toward SARS-CoV-2 via Targeting Virus-Host Interactome. *Front. Genet.* **2021**, *12*, 728960. [CrossRef]
49. Yancey, P.H. Organic osmolytes as compatible, metabolic and counteracting cytoprotectants in high osmolarity and other stresses. *J. Exp. Biol.* **2005**, *208*, 2819–2830. [CrossRef]
50. Zhao, G.; He, F.; Wu, C.; Li, P.; Li, N.; Deng, J.; Zhu, G.; Ren, W.; Peng, Y. Betaine in Inflammation: Mechanistic Aspects and Applications. *Front. Immunol.* **2018**, *9*, 1070. [CrossRef]